



High angular resolution diffusion-weighted imaging in mild traumatic brain injury



Mehrbod Mohammadian^{a,b,*}, Timo Roine^c, Jussi Hirvonen^{a,b,d}, Timo Kurki^{a,b,d}, Henna Ala-Seppälä^a, Janek Frantzén^{a,e}, Ari Katila^f, Anna Kyllönen^a, Henna-Riikka Maanpää^a, Jussi Posti^{a,b,e}, Riikka Takala^f, Jussi Tallus^a, Olli Tenovuo^{a,b}

^aDepartment of Neurology, University of Turku, Turku, Finland

^bDivision of Clinical Neurosciences, Department of Rehabilitation and Brain Trauma, Turku University Hospital, Turku, Finland

^ciMinds-Vision lab, Department of Physics, University of Antwerp, Antwerp, Belgium

^dDepartment of Radiology, Turku University Hospital, Turku, Finland

^eDivision of Clinical Neurosciences, Department of Neurosurgery, Turku University Hospital, Turku, Finland

^fPerioperative Services, Intensive Care Medicine and Pain Management, Turku University Hospital and University of Turku, Turku, Finland

ARTICLE INFO

Article history:

Received 9 August 2016

Received in revised form 24 October 2016

Accepted 16 November 2016

Available online 17 November 2016

Keywords:

Traumatic brain injury

Magnetic resonance imaging

Diffusion-weighted magnetic resonance imaging

Probabilistic tractography

Global approach

ABSTRACT

We sought to investigate white matter abnormalities in mild traumatic brain injury (mTBI) using diffusion-weighted magnetic resonance imaging (DW-MRI). We applied a global approach based on tract-based spatial statistics skeleton as well as constrained spherical deconvolution tractography.

DW-MRI was performed on 102 patients with mTBI within two months post-injury and 30 control subjects.

A robust global approach considering only the voxels with a single-fiber configuration was used in addition to global analysis of the tract skeleton and probabilistic whole-brain tractography. In addition, we assessed whether the microstructural parameters correlated with age, time from injury, patient's outcome and white matter MRI hyperintensities. We found that whole-brain global approach restricted to single-fiber voxels showed significantly decreased fractional anisotropy (FA) ($p = 0.002$) and increased radial diffusivity ($p = 0.011$) in patients with mTBI compared with controls. The results restricted to single-fiber voxels were more significant and reproducible than those with the complete tract skeleton or the whole-brain tractography. FA correlated with patient outcomes, white matter hyperintensities and age. No correlation was observed between FA and time of scan post-injury. In conclusion, the global approach could be a promising imaging biomarker to detect white matter abnormalities following traumatic brain injury.

© 2016 The Authors. Published by Elsevier Inc. This is an open access article under the CC BY-NC-ND license (<http://creativecommons.org/licenses/by-nc-nd/4.0/>).

1. Introduction

Traumatic brain injury (TBI) may become one of the main causes of death and disability by 2020 according to World Health Organization (Hyder et al., 2007). Approximately 80% of all TBI cases are considered to be mild (mTBI) (Bazarian et al., 2005). mTBI causes symptoms from transient post-concussion syndrome to long-term morbidity (Sigurdardottir et al., 2009). Even though the majority of the patients with mTBI eventually recover completely, half of patients develop

neurocognitive problems within the first month and almost one-fourth may have residual symptoms at one year (McMahon et al., 2014). The current clinical and imaging determinants insufficiently correlate with incidence of posttraumatic sequels in patients with mTBI. Common neuroimaging techniques such as computed tomography and conventional magnetic resonance imaging (MRI) have been widely used in TBI to detect macroscopic changes in the brain (Shenton et al., 2012), but they often fail to show diffuse axonal injury (DAI) (Mechtler et al., 2014; Shenton et al., 2012). Diffusion-weighted (DW) MRI is capable of showing white matter abnormalities not visible in routine MRI due to its sensitivity to microstructural changes. Diffusion tensor imaging (DTI) (Basser et al., 1994a, 1994b), which is commonly used to study white matter pathology non-invasively (Xu et al., 2007) has been shown to be sensitive and one of the most promising methods in revealing subtle brain changes in mTBI (Eierud et al., 2014; Shenton et al., 2012).

Several studies have shown that DW-MRI and in particular DTI could be helpful in identifying TBI-related alterations in brain structure (Shetty et al., 2016). Reduced fractional anisotropy (FA) and increased

Abbreviations: AD, axial diffusivity; CSD, constrained-spherical deconvolution; DAI, diffuse axonal injury; DTI, diffusion tensor imaging; DW-MRI, diffusion-weighted magnetic resonance imaging; FA, fractional anisotropy; GCS, Glasgow Coma Scale; GOSe, Glasgow Outcome Scale extended; HARDI, high angular resolution diffusion imaging; MD, mean diffusivity; mTBI, mild traumatic brain injury; PTA, post-traumatic amnesia; RD, radial diffusivity; TBI, traumatic brain injury; TBSS, tract-based spatial statistics.

* Corresponding author at: Department of Neurology, University of Turku, Hämeentie 11, 20521 Turku, Finland.

E-mail address: mehmoh@utu.fi (M. Mohammadian).

mean diffusivity (MD) have been reported in patients with mTBI in acute or sub-acute stage (Aoki et al., 2012; Gu et al., 2013; Kumar et al., 2009; Toth et al., 2013; Wilde et al., 2008). DTI findings in acute and sub-acute phase of mTBI have been related to clinical outcome (Edlow et al., 2016; Messé et al., 2011; Yuh et al., 2014). However, DTI is not yet widely used as an imaging biomarker of TBI in clinical practice.

Moreover, although DTI is a useful tool for detection of changes in brain white matter, it has its inherent limitations (Jones and Cercignani, 2010; Tournier et al., 2011) and there are inconsistencies in results with regard to DTI measurements such as FA and MD in TBI (Lin et al., 2015). DTI can only model Gaussian diffusion while not all diffusion processes that occur in the brain are Gaussian (Bammer et al., 2003). Crossing fibers, present in the majority of white matter voxels (Jeurissen et al., 2013), are an issue that cannot be addressed by DTI. By utilizing DTI, results will yield lower FA values in voxels with complex fiber configurations. High angular resolution diffusion imaging methods have been developed to overcome these shortcomings (Descoteaux and Deriche, 2015; Tournier et al., 2011). Constrained-spherical deconvolution (CSD) is one of these methods, and is shown to be a robust way to resolve the crossing fiber issue associated with DTI (Farquharson et al., 2013; Tournier et al., 2004, 2007). In this study, we used a robust global approach (Hsu et al., 2012; Roine et al., 2013) by calculating mean anisotropy and diffusivity measures in the whole brain and CSD-based tractography (Jeurissen et al., 2011) to investigate microstructural abnormalities within two months of mTBI. CSD-based tractography has recently been in use to investigate abnormalities and network alterations following mTBI (van der Horn et al., 2016). We restricted the analysis to voxels with a single fiber orientation in order to remove the confounding effect of fiber complexity (Jeurissen et al., 2013; Tax et al., 2015; Vos et al., 2011) and to investigate changes in voxels with higher FA values than normal DTI between patients and controls.

2. Materials and methods

2.1. Subjects

During the EU-funded international TBICare (Evidence-based Diagnostic and Treatment Planning Solution for Traumatic Brain Injuries) project, 102 prospectively recruited patients with acute or sub-acute mTBI (age 47 ± 20) underwent DW-MRI in Turku, Finland within two months post-injury (21.2 ± 14.9 days) (Table 1). In addition, 30 control subjects with acute orthopedic injuries without acute or previous brain disorders (age 50 ± 20) were recruited (Table 1). The participants gave written informed consent, and the study was approved by the Ethical Committee of the Hospital district of South-West Finland. Patients with TBI were recruited using wide inclusion and few exclusion criteria as previously described (Takala et al., 2015). Glasgow Coma Scale (GCS) was used to assess severity of TBI (Braakman et al., 1980; Teasdale et al., 1978). Patients with $GCS \geq 13$ were further divided into two groups

(≤ 24 or > 24 h) according to the duration of post-traumatic amnesia (PTA). The outcomes of patients with TBI were assessed using Extended Glasgow Outcome Scale (GOSe) that divides patients with TBI into eight groups allowing the standardized assessment of their recovery (Wilson et al., 1998). The outcome assessment was done 3–6 months after the injury. GOSe score was used as an ordinal variable ranging from 1 (death) to 8 (full recovery). For 21 of the control subjects, MRI was repeated later to evaluate reproducibility. Fazekas grading (Fazekas et al., 1987) was used to assess white matter hyperintensities potentially indicative of small vessel disease.

2.2. MR acquisition

MRI data was acquired using a Siemens 3 T MRI scanner (Magnetom Verio 3 T, Siemens Healthcare, Erlangen, Germany). Axial DW-MR images were obtained by a spin-echo echo-planar imaging sequence with repetition time 11.7 s, echo time 106 ms, $2 \times 2 \times 2$ mm voxel size and 77 axial slices; the field of view was 192×192 mm. Diffusion gradients with $b = 1000$ s/mm² were applied in 64 directions uniformly distributed on a unit sphere (Jones et al., 1999).

2.3. Data analysis

The DW-MRI data were analyzed using ExploreDTI (Leemans et al., 2009) and MATLAB (Mathworks, Natick, MA) software. Images were first corrected for motion and eddy current distortions (Leemans and Jones, 2009). Then, white matter FA skeleton was reconstructed based on tract-based spatial statistics (TBSS) (Smith et al., 2006). Fiber orientation distributions were estimated with CSD using spherical harmonics up to order six (Tournier et al., 2004, 2007), and recursive calibration of the single-fiber response function (Tax et al., 2014).

As the microstructural indices based on traditional DTI are affected by the complexity of the fiber configurations, we chose to investigate only the voxels with a single fiber orientation detected by CSD within the white matter skeleton. In addition, we compared these results to the microstructural indices measured within the complete white matter skeleton and the whole-brain fiber tractogram generated with probabilistic CSD-based tractography (Jeurissen et al., 2011). To calculate the mean microstructural values for the whole-brain tractogram, we first constructed a tract density image (Calamante et al., 2010) in diffusion space, which was multiplied voxel-wise with the microstructural values. These values were then added together and divided by the global sum of the tract density image. Seeding was performed using a grid of $1 \times 1 \times 1$ mm³ (8 seeds per voxel) and tractography was terminated using an angular threshold of 45°. Fiber orientation density function amplitude threshold of 0.1 and step size of 1 mm were used for tracking. The thresholds for the length of streamlines in the tractography were from 50 to 500 mm. These parameters resulted in $360,000 \pm 250,000$ streamlines in the patient group and $380,000 \pm 235,000$ streamlines in the control group.

Table 1
Characteristics of the study subjects and injury to MR imaging intervals.

Study group	Number of subjects	Age (years) (mean \pm std) (min-max)	Gender	Imaging time (days) (mean \pm std) (min-max)
mTBI patients ($GCS \geq 13$)	102	47 ± 20 18–84	70 M 32 F	21 ± 15 1–52
mTBI patients ($GCS \geq 13$ & $PTA \leq 24$ h)	78	45 ± 20 18–84	52 M 26 F	21 ± 15 2–51
mTBI patients ($GCS \geq 13$ & $PTA > 24$ h)	24	55 ± 16 20–78	18 M 6 F	21 ± 16 1–52
Controls	30	50 ± 20 22–90	14 M 16 F	

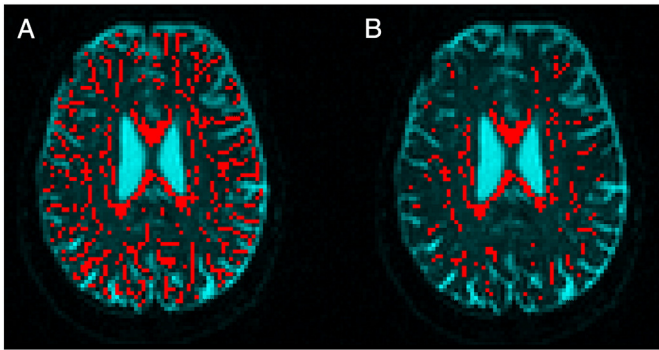


Fig. 1. Illustration of different approaches. (A) FA skeleton. (B) Single fiber voxel selection from the skeletonized FA.

To investigate microstructural white matter properties, global measures of FA, MD, radial diffusivity (RD), and axial diffusivity (AD) were calculated using three different approaches: complete skeleton, single-fiber skeleton (Fig. 1) and whole-brain tractogram. The distribution of these properties within each subject was also calculated. General linear model was then used to test for between group changes in all of the measurements. We applied a repeated measures analysis of variance (rmANOVA) with method as a within-subject factor and group as a between-subject factor. Group by region interaction terms were analyzed to compare different measures in terms of detecting a group difference in FA. Fazekas grading, and age were included in the statistical model as covariates (Ilvesmäki et al., 2014; Lebel et al., 2012; Lee et al., 2010, 2009; Stadlbauer et al., 2008; Yoon et al., 2008). Separate linear models were then created for each method.

In addition, the Pearson correlation coefficients of the microstructural properties with respect to GOS-e, time post-injury and age were calculated. Non-parametric Spearman correlation was used to investigate the correlation of microstructural properties with Fazekas grading.

Statistical analyses were performed using SPSS (version 23, SPSS IBM, New York, NY). For all statistical analysis, confidence interval of 95% was considered for the statistical significance of the results.

Intraclass correlation coefficients (ICC) of the microstructural properties were calculated to evaluate the reproducibility of the methods in control subjects (Owen et al., 2013; Shrout and Fleiss, 1979; Shrout, 1998).

3. Results

3.1. Microstructural white matter abnormalities in mTBI

FA values were significantly lower in patients with mTBI compared to healthy controls ($p = 0.002$), and this difference depended on the

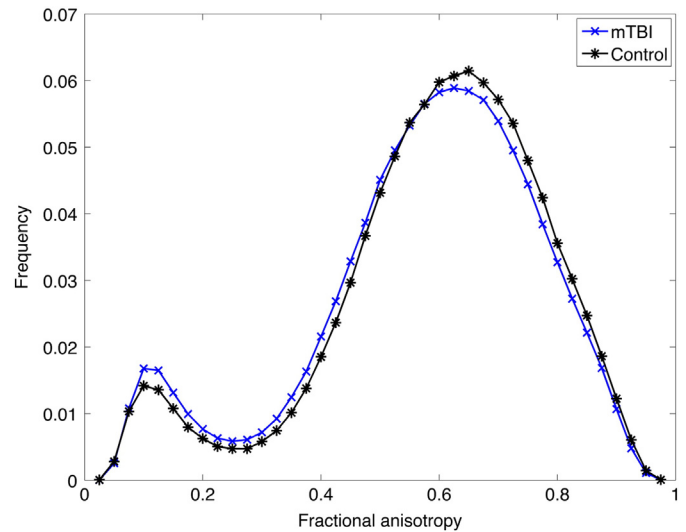


Fig. 2. Histograms of the fractional anisotropy values in patients with mTBI and controls. Histograms of all fractional anisotropy values in patients with acute or sub-acute mild traumatic brain injury, and controls using the single-fiber skeleton approach.

method (group by method interaction, $F = 3.36$, $p = 0.039$). The group difference was statistically significant for each method (Table 2). The difference in FA was significant both in patients with ≤ 24 h of PTA ($p = 0.006$) and those with >24 h of PTA ($p = 0.003$). Group-wise histograms showed that mTBI patients had less voxels with high FA values and more voxels with low FA values compared with controls (Fig. 2). The rmANOVA also indicated significant main effects of group ($F = 8.54$, $p = 0.004$), age ($F = 86.6$, $p < 0.001$), and Fazekas grade ($F = 4.92$, $p = 0.028$).

RD was increased in all patients compared with controls ($p = 0.011$), and separately in patients with PTA ≤ 24 h ($p = 0.033$) and >24 h of PTA ($p = 0.006$). AD and MD did not show significant differences (Table 3). Results without controlling for white matter hyperintensities showed significant differences between patients and controls in FA, MD and RD (Supplementary Tables 1 and 2).

3.2. Comparison of methods

The method restricted to single-fiber skeleton voxels, which constituted 29.13% of the WM skeleton voxels in average, produced the most significant results compared to whole skeleton and whole-brain CSD-based tractogram (Table 2). In addition, the single-fiber method was the most reproducible, as shown by the ICC values calculated from the control subjects (Table 4). Of the microstructural properties, RD and

Table 2
Global fractional anisotropy (FA) values measured with the three different methods in acute or sub-acute mild traumatic brain injury (mTBI defined as GCS ≥ 13 , GCS ≥ 13 and post traumatic amnesia (PTA) ≤ 24 h, GCS ≥ 13 and PTA > 24 h) vs controls. Age and white matter hyperintensities (measured by Fazekas scale) were used as covariates.

Study group	FA skeleton, single-fiber only		FA skeleton		FA tractogram	
	mean \pm SD	F-value (p-value)	mean \pm SD	F-value (p-value)	mean \pm SD	F-value (p-value)
All mTBI (GCS ≥ 13)	0.576 \pm 0.042	9.917	0.412 \pm 0.025	4.606	0.521 \pm 0.047	6.764
Controls	0.591 \pm 0.034	0.002	0.419 \pm 0.021	0.034	0.534 \pm 0.043	0.010
mTBI (GCS ≥ 13 & PTA ≤ 24 h)	0.582 \pm 0.040	7.808	0.416 \pm 0.022	3.195	0.527 \pm 0.048	4.806
Controls	0.591 \pm 0.034	0.006	0.419 \pm 0.021	0.077	0.534 \pm 0.043	0.031
mTBI (GCS ≥ 13 & PTA > 24 h)	0.556 \pm 0.042	9.497	0.399 \pm 0.030	5.954	0.501 \pm 0.040	6.565
Controls	0.591 \pm 0.034	0.003	0.419 \pm 0.021	0.018	0.534 \pm 0.043	0.013

Table 3

Global mean (MD), axial (AD) and radial (RD) diffusivity values measured with the single-fiber skeleton approach in acute or sub-acute mild traumatic brain injury (mTBI defined as GCS \geq 13, GCS \geq 13 and post traumatic amnesia (PTA) \geq 24 h, GCS \geq 13 and PTA > 24 h) vs controls. Age and white matter hyperintensities (measured by Fazekas scale) were used as covariates.

Study group	MD ($\times 10^{-3}$ mm ² /s)		AD ($\times 10^{-3}$ mm ² /s)		RD ($\times 10^{-3}$ mm ² /s)	
	mean \pm SD	F-value (p-value)	mean \pm SD	F-value (p-value)	mean \pm SD	F-value (p-value)
All mTBI (GCS \geq 13) Controls	0.783 \pm 0.073 0.765 \pm 0.058	2.801 0.097	1.389 \pm 0.081 1.368 \pm 0.073	1.528 0.219	0.560 \pm 0.105 0.525 \pm 0.085	6.672 0.011
mTBI (GCS \geq 13 & PTA \leq 24 h) Controls	0.775 \pm 0.073 0.765 \pm 0.058	1.677 0.198	1.383 \pm 0.083 1.368 \pm 0.073	0.808 0.371	0.546 \pm 0.103 0.525 \pm 0.085	4.671 0.033
mTBI (GCS \geq 13 & PTA > 24 h) Controls	0.809 \pm 0.066 0.765 \pm 0.058	3.99 0.051	1.411 \pm 0.074 1.368 \pm 0.073	2.403 0.127	0.604 \pm 0.103 0.525 \pm 0.085	8.087 0.006

Table 4

Reproducibility measured with intraclass correlation coefficient (ICC) of the global microstructural properties (In 21 control subjects with repeated scans). FA: fractional anisotropy; MD: mean diffusivity; RD: radial diffusivity; AD: axial diffusivity.

Microstructural property	ICC
FA, single-fiber skeleton	0.970
FA, whole skeleton	0.920
FA, tractogram	0.958
MD, single-fiber skeleton	0.939
RD, single-fiber skeleton	0.979
AD, single-fiber skeleton	0.863

FA were the most reproducible measures. The histograms showed that single-fiber method produced higher mean FA values than whole-brain tractogram or the complete skeleton (Fig. 3).

3.3. Correlation of white matter properties to age, time of scan post-injury, patient's outcome and white matter hyperintensities

FA did not correlate significantly with post-injury scan delay in patients with GCS \geq 13 ($p = 0.899$ in all patients, $p = 0.535$ in patients with ≤ 24 h of PTA and $p = 0.170$ in patients with > 24 h of PTA), although it was negatively associated with age ($p < 0.0001$ in all patients and also in both patient groups divided by the duration of PTA) and

positively associated with GOSe ($p = 0.0003$ in all patients and $p = 0.004$ in patients with ≤ 24 h of PTA) (Table 5). In addition, FA correlated negatively with Fazekas grading ($p < 0.0001$ in all patients and patients with ≤ 24 h of PTA). No statistically significant correlation was observed between FA and GOSe ($p = 0.311$) and FA and Fazekas ($p = 0.092$) in patients with > 24 h of PTA. On average, patients had more white matter hyperintensities than controls ($p = 0.015$). Nevertheless, our main analysis controlled for this potential confounder in the statistical model.

4. Discussion

We found lower white matter FA values in patients with mTBI compared with controls, consistent with white matter damage. FA values were also associated with mTBI outcome measured using the GOSe, although this correlation was not statistically significant in patients with > 24 h of PTA. Importantly, the group difference depended on the analysis method, such that the global whole-brain approach based on TBSS skeleton and restricted to single-fiber voxels using CSD had the best sensitivity to detect this difference and it was also the most reproducible. This method may have clinical utility in aiding the diagnostics of mTBI.

Our findings of decreased FA and increased MD, RD and AD in patients with mTBI compared to controls is in accordance with previous studies in acute or sub-acute phase of mTBI (Arfanakis et al., 2002; Gray et al., 2013; Messé et al., 2011; Miles et al., 2008; Narayana et al., 2014; Rutgers et al., 2008; Toth et al., 2013). The use of white matter

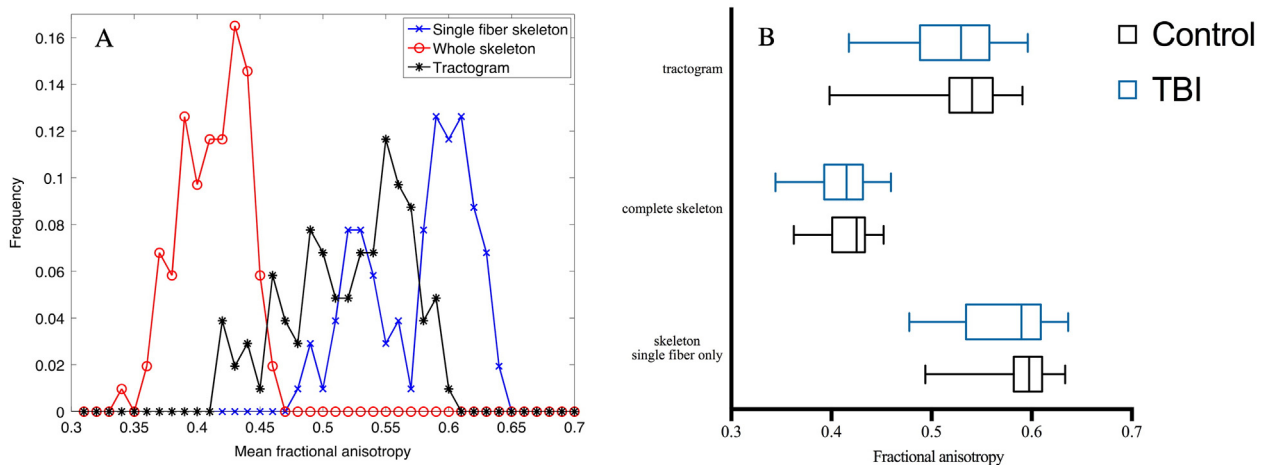


Fig. 3. Differences in fractional anisotropy between the three approaches. (A) Histograms of mean fractional anisotropy values using the single-fiber skeleton, whole skeleton and tractography approaches in acute or sub-acute mild traumatic brain injury (mTBI). (B) Boxplot of FA values in patients and controls yielded by three approaches: complete white matter skeleton, white matter skeleton restricted to single-fiber voxels and whole brain tractogram. (This graph was generated by GraphPad Prism version 7.0, GraphPad Software, San Diego, California, USA, www.graphpad.com).

Table 5
Pearson correlation coefficients of fractional anisotropy (FA) with neurological outcome measured with Glasgow Outcome Scale extended (GOSe), white matter hyperintensities measured, time post-injury, and age as well as non-parametric Spearman correlation coefficient of FA with Fazekas. Two-tailed significance was used to test the statistically significant correlation ($p < 0.05$).

Study group	FA and GOSe	FA and Fazekas	FA and time	FA and age
All mTBI (n = 102)	r = 0.363 p = 0.0003	r = -0.619 p < 0.0001	r = -0.013 p = 0.899	r = -0.787 p < 0.0001
mTBI with PTA ≤ 24 h (n = 78)	r = 0.341 p = 0.004	r = -0.646 p < 0.0001	r = 0.071 p = 0.535	r = -0.814 p < 0.0001
mTBI with PTA > 24 h (n = 24)	r = 0.227 p = 0.311	r = -0.352 p = 0.092	r = -0.289 p = 0.170	r = -0.639 p < 0.001

skeleton minimizes the effect of isotropic partial volume effects, shown to affect CSD (Roine et al., 2014, 2015a) and DTI (Alexander et al., 2001), but has other inherent limitations (Bach et al., 2014). However, these limitations are largely related to registration problems, which could be eliminated by applying a global whole-brain wide approach. In addition, the robustness of our findings was further demonstrated by their replication with CSD-based whole-brain tractography, which avoids most of the limitations of the skeletonization.

Our findings of increased diffusivity and reduced anisotropy may indicate extracellular brain edema (Iffland et al., 2014; Veeramuthu et al., 2015), axonal degradation (Beaulieu, 2002), or demyelination (Song et al., 2002) of white matter structures affecting their integrity. It has been shown that at the acute stage of the injury, the axonal degradation is the primary pathology (Mac Donald et al., 2007) while demyelination, which can be the cause of the increase in RD is the major pathological change after the acute stage (Mac Donald et al., 2007; Song et al., 2005).

Patients with longer duration of PTA tended to have lower anisotropy and higher diffusivity values compared to patients with shorter PTA. However, the differences between these two severity groups were not statistically significant.

Whole-brain histograms demonstrated that the difference in mean FA between the controls and patients with mTBI manifests as both higher number of low FA values and lower number of high FA values in the histogram. Previously, whole-brain histogram analysis did not differentiate between mTBI patients and controls (Inglese et al., 2005), suggesting that white matter microstructural abnormalities may be too subtle to be detected with DTI. However, the previous study had only six gradient directions and the analysis included all gray and white matter voxels within the brain (Inglese et al., 2005).

A recent study showed no local white matter changes in acute mTBI compared to controls (Ilvesmäki et al., 2014). In that study, MRI was performed on the average 48 h post-injury, while our MR imaging was done at a mean of 21.3 days post-injury. These differing results suggest that white matter changes develop slowly and may not be measurable immediately after injury. In addition, our robust global approach and elimination of complex fiber configurations compared to their voxel-based approach could account for the differences in these studies.

A limitation of this study is that the b-value describing the amount of diffusion weighting was lower than optimal for CSD-based tractography (Tournier et al., 2013). However, 64 gradient orientations were likely sufficient and crossing fibers could reliably be detected as previously shown in e.g. (Annen et al., 2016; Roine et al., 2015b, 2015c). In addition, patients in both acute and sub-acute stages of mTBI were included in this study, which might have affected the results although within this time range our results did not correlate with the time from injury. Finally, patients with mTBI tended to have higher incidence of white matter hyperintensities, which is a potential confounder in assessing mTBI-related alterations in mTBI. However, these visible white matter changes may also be related to the mTBI and additionally we controlled for this potential confounder in the statistical models.

In conclusion, our study shows that mTBI is associated with microstructural changes in the white matter and that these changes correlate with the outcome. As a novel finding, we show that a single-fiber approach improves the sensitivity and reliability in detecting these alterations.

Supplementary data to this article can be found online at <http://dx.doi.org/10.1016/j.nicl.2016.11.016>.

Conflicts of interest declaration

The authors report no conflicts of interest.

Funding

This study was partly funded by the European Commission under the 7th Framework Programme (FP7-270259-TBicare). M.M received funding from University of Turku and T.R received support from the Instrumentarium Scientific Foundation, Finland and Maud Kuistila Memorial Foundation, Finland.

Acknowledgements

No acknowledgements.

References

- Alexander, A.L., Hasan, K.M., Lazar, M., Tsuruda, J.S., Parker, D.L., 2001. Analysis of partial volume effects in diffusion-tensor MRI. *Magn. Reson. Med.* 45:770–780. <http://dx.doi.org/10.1002/mrm.1105>.
- Annen, J., Heine, L., Ziegler, E., Frasso, G., Bahri, M., Di Perri, C., Stender, J., Martial, C., Wannez, S., D'ostilio, K., Amico, E., Antonopoulos, G., Bernard, C., Tshibanda, F., Hustinx, R., Laureys, S., 2016. Function-structure connectivity in patients with severe brain injury as measured by MRI-DWI and FDG-PET. *Hum. Brain Mapp.* <http://dx.doi.org/10.1002/hbm.23269>.
- Aoki, Y., Inokuchi, R., Gunshin, M., Yahagi, N., Suwa, H., 2012. Diffusion tensor imaging studies of mild traumatic brain injury: a meta-analysis. *J. Neurol. Neurosurg. Psychiatry* 83:870–876. <http://dx.doi.org/10.1136/jnnp-2012-302742>.
- Arfanakis, K., Haughton, V.M., Carew, J.D., Rogers, B.P., Dempsey, R.J., Meyerand, M.E., 2002. Diffusion tensor MR imaging in diffuse axonal injury. *AJNR Am. J. Neuroradiol.* 23, 794–802.
- Bach, M., Laun, F.B., Leemans, A., Tax, C.M.W., Biessels, G.J., Stieltjes, B., Maier-Hein, K.H., 2014. Methodological considerations on tract-based spatial statistics (TBSS). *NeuroImage* 100:358–369. <http://dx.doi.org/10.1016/j.neuroimage.2014.06.021>.
- Bammer, R., Acar, B., Moseley, M.E., 2003. In vivo MR tractography using diffusion imaging. *Eur. J. Radiol.* 45:223–234. [http://dx.doi.org/10.1016/S0720-048X\(02\)00311-X](http://dx.doi.org/10.1016/S0720-048X(02)00311-X).
- Basser, P.J., Mattiello, J., LeBihan, D., 1994a. MR diffusion tensor spectroscopy and imaging. *Biophys. J.* 66:259–267. [http://dx.doi.org/10.1016/S0006-3495\(94\)80775-1](http://dx.doi.org/10.1016/S0006-3495(94)80775-1).
- Basser, P.J., Mattiello, J., LeBihan, D., 1994b. Estimation of the effective self-diffusion tensor from the NMR spin echo. *J. Magn. Reson. B* 103:247–254. <http://dx.doi.org/10.1006/jmrb.1994.1037>.
- Bazarian, J.J., McClung, J., Shah, M.N., Cheng, Y.T., Flesher, W., Kraus, J., 2005. Mild traumatic brain injury in the United States, 1998–2000. *Brain Inj.* 19:85–91. <http://dx.doi.org/10.1080/02699050410001720158>.
- Beaulieu, C., 2002. The basis of anisotropic water diffusion in the nervous system - a technical review. *NMR Biomed.* <http://dx.doi.org/10.1002/nbm.782>.
- Braakman, R., Gelpke, G.J., Habbema, J.D.F., Maas, A.L.R., Minderhoud, J.M., 1980. Systematic selection of prognostic features in patients with severe head injury. *Neurosurgery* 6, 362–370 (doi:No DOI).

- Calamante, F., Tournier, J.D., Jackson, G.D., Connelly, A., 2010. Track-density imaging (TDI): super-resolution white matter imaging using whole-brain track-density mapping. *NeuroImage* 53:1233–1243. <http://dx.doi.org/10.1016/j.neuroimage.2010.07.024>.
- Descoteaux, M., Deriche, R., 2015. From local Q-ball estimation to fibre crossing tractography. *Handbook of Biomedical Imaging*. Springer US, Boston, MA: pp. 455–473 http://dx.doi.org/10.1007/978-0-387-09749-7_25.
- Edlow, B.L., Copen, W.A., Izzy, S., Bakhadirov, K., van der Kouwe, A., Glenn, M.B., Greenberg, S.M., Greer, D.M., Wu, O., 2016. Diffusion tensor imaging in acute-to-subacute traumatic brain injury: a longitudinal analysis. *BMC Neurol.* 16:2. <http://dx.doi.org/10.1186/s12883-015-0525-8>.
- Eierud, C., Craddock, R.C., Fletcher, S., Aulakh, M., King-Casas, B., Kuehl, D., LaConte, S.M., 2014. Neuroimaging after mild traumatic brain injury: review and meta-analysis. *NeuroImage Clin.* 4:283–294. <http://dx.doi.org/10.1016/j.nicl.2013.12.009>.
- Farquharson, S., Tournier, J.-D., Calamante, F., Fabin, G., Schneider-Kolsky, M., Jackson, G.D., Connelly, A., 2013. White matter fiber tractography: why we need to move beyond DTI. *J. Neurosurg.* 118:1367–1377. <http://dx.doi.org/10.3171/2013.2.JNS121294>.
- Fazekas, F., Chawluk, J.B., Alavi, A., 1987. MR signal abnormalities at 1.5 T in Alzheimer's dementia and normal aging. *Am. J. Neuroradiol.* <http://dx.doi.org/10.2214/ajr.149.2.351>.
- Gray, K.R., Aljabar, P., Heckemann, R.A., Hammers, A., Rueckert, D., 2013. Random forest-based similarity measures for multi-modal classification of Alzheimer's disease. *NeuroImage* 65:167–175. <http://dx.doi.org/10.1016/j.neuroimage.2012.09.065>.
- Gu, L., Li, J., Feng, D.-F., Cheng, E.-T., Li, D.-C., Yang, X.-Q., Wang, B.-C., 2013. Detection of white matter lesions in the acute stage of diffuse axonal injury predicts long-term cognitive impairments: a clinical diffusion tensor imaging study. *J. Trauma Acute Care Surg.* 74:242–247. <http://dx.doi.org/10.1097/TA.0b013e3182684fe8>.
- Hsu, J.-L., Chen, Y.-L., Leu, J.-G., Jaw, F.-S., Lee, C.-H., Tsai, Y.-F., Hsu, C.-Y., Bai, C.-H., Leemans, A., 2012. Microstructural white matter abnormalities in type 2 diabetes mellitus: a diffusion tensor imaging study. *NeuroImage* 59:1098–1105. <http://dx.doi.org/10.1016/j.neuroimage.2011.09.041>.
- Hyder, A.A., Wunderlich, C.A., Puvanachandra, P., Gururaj, G., Kobusingye, O.C., 2007. The impact of traumatic brain injuries: a global perspective. *NeuroRehabilitation* 22, 341–353 (doi:<http://iospress.metapress.com/content/103177?sortorder=asc>).
- Iffland, P.H., Grant, G.A., Janigro, D., 2014. Mechanisms of cerebral edema leading to early seizures after traumatic brain injury. In: Lo, E.H., Lok, J., Ning, M., Whalen, M.J. (Eds.), *Vascular Mechanisms in CNS Trauma*, pp. 29–45 (New York).
- Ivlesmäki, T., Luoto, T.M., Hakulinen, U., Brander, A., Ryymin, P., Eskola, H., Iverson, G.L., Ohman, J., 2014. Acute mild traumatic brain injury is not associated with white matter change on diffusion tensor imaging. *Brain* 137:1876–1882. <http://dx.doi.org/10.1093/brain/awu095>.
- Inglese, M., Makani, S., Johnson, G., Cohen, B.A., Silver, J.A., Gonen, O., Grossman, R.I., 2005. Diffuse axonal injury in mild traumatic brain injury: a diffusion tensor imaging study. *J. Neurosurg.* 103:298–303. <http://dx.doi.org/10.3171/jns.2005.103.2.0298>.
- Jeurissen, B., Leemans, A., Jones, D.K., Tournier, J.D., Sijbers, J., 2011. Probabilistic fiber tracking using the residual bootstrap with constrained spherical deconvolution. *Hum. Brain Mapp.* <http://dx.doi.org/10.1002/hbm.21032>.
- Jeurissen, B., Leemans, A., Tournier, J.D., Jones, D.K., Sijbers, J., 2013. Investigating the prevalence of complex fiber configurations in white matter tissue with diffusion magnetic resonance imaging. *Hum. Brain Mapp.* 34:2747–2766. <http://dx.doi.org/10.1002/hbm.22099>.
- Jones, D.K., Cercignani, M., 2010. Twenty-five pitfalls in the analysis of diffusion MRI data. *NMR Biomed.* <http://dx.doi.org/10.1002/nbm.1543>.
- Jones, D.K., Horsfield, M.A., Simmons, A., 1999. Optimal strategies for measuring diffusion in anisotropic systems by magnetic resonance imaging. *Magn. Reson. Med.* 42: 515–525. [http://dx.doi.org/10.1002/\(SICI\)1522-2594\(199909\)42:3<515::AID-MRM14-3.0.CO;2-Q](http://dx.doi.org/10.1002/(SICI)1522-2594(199909)42:3<515::AID-MRM14-3.0.CO;2-Q).
- Kumar, R., Gupta, R.K., Husain, M., Chaudhry, C., Srivastava, A., Saksena, S., Rathore, R.K.S., 2009. Comparative evaluation of corpus callosum DTI metrics in acute mild and moderate traumatic brain injury: its correlation with neuropsychometric tests. *Brain Inj.* 23:675–685. <http://dx.doi.org/10.1080/02699050903014915>.
- Lebel, C., Gee, M., Camicioli, R., Wieler, M., Martin, W., Beaulieu, C., 2012. Diffusion tensor imaging of white matter tract evolution over the lifespan. *NeuroImage* 60:340–352. <http://dx.doi.org/10.1016/j.neuroimage.2011.11.094>.
- Lee, D.Y., Fletcher, E., Martinez, O., Ortega, M., Zozulya, N., Kim, J., Tran, J., Buonocore, M., Carmichael, O., Decarli, C., 2009. Regional pattern of white matter microstructural changes in normal aging, MCI, and AD. *Neurology* 73:1722–1728. <http://dx.doi.org/10.1212/WNL.0b013e3181c33afb>.
- Lee, D.Y., Fletcher, E., Martinez, O., Zozulya, N., Kim, J., Tran, J., Buonocore, M., Carmichael, O., Decarli, C., 2010. Vascular and degenerative processes differentially affect regional interhemispheric connections in normal aging, mild cognitive impairment, and Alzheimer disease. *Stroke* 41:1791–1797. <http://dx.doi.org/10.1161/STROKEAHA.110.582163>.
- Leemans, A., Jones, D.K., 2009. The B-matrix must be rotated when correcting for subject motion in DTI data. *Magn. Reson. Med.* 61:1336–1349. <http://dx.doi.org/10.1002/mrm.21890>.
- Leemans, A., Jeurissen, B., Sijbers, J., Jones, D., 2009. ExploreDTI: a graphical toolbox for processing, analyzing, and visualizing diffusion MR data. *Proceedings 17th Scientific Meeting, International Society for Magnetic Resonance in Medicine*, p. 3537.
- Lin, M., He, H., Schifitto, G., Zhong, J., 2015. Simulation of changes in diffusion related to different pathologies at cellular level after traumatic brain injury. *Magn. Reson. Med.* <http://dx.doi.org/10.1002/mrm.25816>.
- Mac Donald, C.L., Dickranian, K., Bayly, P., Holtzman, D., Brody, D., 2007. Diffusion tensor imaging reliably detects experimental traumatic axonal injury and indicates approximate time of injury. *J. Neurosci.* 27:11869–11876. <http://dx.doi.org/10.1523/JNEUROSCI.3647-07.2007>.
- McMahon, P., Hricik, A., Yue, J.K., Puccio, A.M., Inoue, T., Lingsma, H.F., Beers, S.R., Gordon, W.A., Valadka, A.B., Manley, G.T., Okonkwo, D.O., Investigators, T.R.A.C.K.-T.B.I., 2014. Symptomatology and functional outcome in mild traumatic brain injury: results from the prospective TRACK-TBI study. *J. Neurotrauma* 31:26–33. <http://dx.doi.org/10.1089/neu.2013.2984>.
- Mechter, L.L., Shastri, K.K., Crutchfield, K.E., 2014. Advanced neuroimaging of mild traumatic brain injury. *Neurol. Clin.* <http://dx.doi.org/10.1016/j.ncl.2013.08.002>.
- Messé, A., Caplain, S., Parodot, G., Garrigue, D., Mineo, J.F., Soto Ares, G., Ducreux, D., Vignaud, F., Rozec, G., Desal, H., Péligrini-Issac, M., Montreuil, M., Benali, H., Lehericy, S., 2011. Diffusion tensor imaging and white matter lesions at the subacute stage in mild traumatic brain injury with persistent neurobehavioral impairment. *Hum. Brain Mapp.* 32:999–1011. <http://dx.doi.org/10.1002/hbm.21092>.
- Miles, L., Grossman, R.I., Johnson, G., Babb, J.S., Diller, L., Inglese, M., 2008. Short-term DTI predictors of cognitive dysfunction in mild traumatic brain injury. *Brain Inj.* 22: 115–122. <http://dx.doi.org/10.1080/02699050801888816>.
- Narayana, P.A., Yu, X., Hasan, K.M., Wilde, E.A., Levin, H.S., Hunter, J.V., Miller, E.R., Patel, V.K.S., Robertson, C.S., McCarthy, J.J., 2014. Multi-modal MRI of mild traumatic brain injury. *NeuroImage Clin.* <http://dx.doi.org/10.1016/j.nicl.2014.07.010>.
- Owen, J.P., Ziv, E., Bukshpun, P., Pojman, N., Wakahiro, M., Berman, J.L., Roberts, T.P.L., Friedman, E.J., Sherr, E.H., Mukherjee, P., 2013. Test-retest reliability of computational network measurements derived from the structural connectome of the human brain. *Brain Connect.* 3:160–176. <http://dx.doi.org/10.1089/brain.2012.0121>.
- Roine, U., Roine, T., Salmi, J., Nieminen-Von Wendt, T., Leppämäki, S., Rintahaka, P., Tani, P., Leemans, A., Sams, M., 2013. Increased coherence of white matter fiber tract organization in adults with asperger syndrome: a diffusion tensor imaging study. *Autism Res.* 6:642–650. <http://dx.doi.org/10.1002/aur.1332>.
- Roine, T., Jeurissen, B., Perrone, D., Aelterman, J., Leemans, A., Philips, W., Sijbers, J., 2014. Isotropic non-white matter partial volume effects in constrained spherical deconvolution. *Front. Neuroinform.* 8:28. <http://dx.doi.org/10.3389/fninf.2014.00028>.
- Roine, U., Roine, T., Salmi, J., Nieminen-von Wendt, T., Tani, P., Leppämäki, S., Rintahaka, P., Caeyenberghs, K., Leemans, A., Sams, M., 2015a. Abnormal wiring of the connectome in adults with high-functioning autism spectrum disorder. *Mol. Autism* 6:65. <http://dx.doi.org/10.1186/s13229-015-0058-4>.
- Roine, U., Salmi, J., Roine, T., Wendt, T.N., Leppämäki, S., Rintahaka, P., Tani, P., Leemans, A., Sams, M., 2015b. Constrained spherical deconvolution-based tractography and tract-based spatial statistics show abnormal microstructural organization in asperger syndrome. *Mol. Autism* 6:4. <http://dx.doi.org/10.1186/2040-2392-6-4>.
- Roine, T., Jeurissen, B., Perrone, D., Aelterman, J., Philips, W., Leemans, A., Sijbers, J., 2015c. Informed constrained spherical deconvolution (iCSD). *Med. Image Anal.* 24:269–281. <http://dx.doi.org/10.1016/j.media.2015.01.001>.
- Rutgers, D.R., Fillard, P., Parodot, G., Tadie, M., Lasjaunias, P., Ducreux, D., 2008. Diffusion tensor imaging characteristics of the corpus callosum in mild, moderate, and severe traumatic brain injury. *Am. J. Neuroradiol.* 29:1730–1735 (doi: [ajnr.A1213](http://dx.doi.org/10.3171/ajnr.A1213) | pii:[10.3171/ajnr.A1213](http://dx.doi.org/10.3171/ajnr.A1213)).
- Shenton, M.E., Hamoda, H.M., Schneiderman, J.S., Bouix, S., Pasternak, O., Rathi, Y., Vu, M.A., Purohit, M.P., Helmer, K., Koerte, I., Lin, A.P., Westin, C.F., Kikinis, R., Kubicki, M., Stern, R.A., Zafonte, R., 2012. A review of magnetic resonance imaging and diffusion tensor imaging findings in mild traumatic brain injury. *Brain Imaging Behav.* 6: 137–192. <http://dx.doi.org/10.1007/s11682-012-9156-5>.
- Shetty, T., Rance, A., Manning, E., Tsiouris, A.J., 2016. Imaging in chronic traumatic encephalopathy and traumatic brain injury. *Sports Health* 8:26–36. <http://dx.doi.org/10.1177/1941738115588745>.
- Shrout, P.E., 1998. Measurement reliability and agreement in psychiatry. *Stat. Methods Med. Res.* 7:301–317. <http://dx.doi.org/10.1191/096228098672090967>.
- Shrout, P.E., Fleiss, J.L., 1979. Intraclass correlations: uses in assessing rater reliability. *Psychol. Bull.* <http://dx.doi.org/10.1037/0033-2909.86.2.420>.
- Sigurdardottir, S., Andelic, N., Roe, C., Jerstad, T., Schanke, A.-K., 2009. Post-concussion symptoms after traumatic brain injury at 3 and 12 months post-injury: a prospective study. *Brain Inj.* 23:489–497. <http://dx.doi.org/10.1080/02699050902926309>.
- Smith, S.M., Jenkinson, M., Johansen-Berg, H., Rueckert, D., Nichols, T.E., Mackay, C.E., Watkins, K.E., Ciccarelli, O., Cader, M.Z., Matthews, P.M., Behrens, T.E.J., 2006. Tract-based spatial statistics: voxelwise analysis of multi-subject diffusion data. *NeuroImage* 31:1487–1505. <http://dx.doi.org/10.1016/j.neuroimage.2006.02.024>.
- Song, S.-K., Sun, S.-W., Ramsbottom, M.J., Chang, C., Russell, J., Cross, A.H., 2002. Demyelination revealed through MRI as increased radial (but unchanged axial) diffusion of water. *NeuroImage* 17:1429–1436. <http://dx.doi.org/10.1006/nimg.2002.1267>.
- Song, S.-K., Yoshino, J., Le, T.Q., Lin, S.-J., Sun, S.-W., Cross, A.H., Armstrong, R.C., 2005. Demyelination increases radial diffusivity in corpus callosum of mouse brain. *NeuroImage* 26:132–140. <http://dx.doi.org/10.1016/j.neuroimage.2005.01.028>.
- Stadlbauer, A., Salomonowitz, E., Strunk, G., Hammen, T., Ganslandt, O., 2008. Age-related degradation in the central nervous system: assessment with diffusion-tensor imaging and quantitative fiber tracking. *Radiology* 247:179–188. <http://dx.doi.org/10.1148/radiol.2471070707>.
- Takala, R.S., Posti, J.P., Runtti, H., Newcombe, V.F., Outtrim, J., Katila, A.J., Frantzen, J., Ala-Seppälä, H., Kyllönen, A., Maanpää, H.-R., Tallus, J., Hossain, M.I., Coles, J.P., Hutchinson, P., van Gils, M., Menon, D.K., Tenovu, O., 2015. GFAP and UCH-L1 as outcome predictors in traumatic brain injury. *World Neurosurg.* <http://dx.doi.org/10.1016/j.wneu.2015.10.066>.
- Tax, C.M.W., Jeurissen, B., Vos, S.B., Viergever, M.A., Leemans, A., 2014. Recursive calibration of the fiber response function for spherical deconvolution of diffusion MRI data. *NeuroImage* 86:67–80. <http://dx.doi.org/10.1016/j.neuroimage.2013.07.067>.

- Tax, C.M.W., Novikov, D.S., Garyfallidis, E., Viergever, M.A., Descoteaux, M., Leemans, A., 2015. Localizing and characterizing single fiber populations throughout the brain. Proc. 23rd Annual Meeting ISMRM, Toronto, Canada, p. 473.
- Teasdale, G., Knill-Jones, R., van der Sande, J., 1978. Observer variability in assessing impaired consciousness and coma. *J. Neurol. Neurosurg. Psychiatry* 41:603–610. <http://dx.doi.org/10.1136/jnnp.41.7.603>.
- Toth, A., Kovacs, N., Perlaki, G., Orsi, G., Aradi, M., Komaromy, H., Ezer, E., Bukovics, P., Farkas, O., Janszky, J., Doczi, T., Buki, A., Schwarcz, A., 2013. Multi-modal magnetic resonance imaging in the acute and sub-acute phase of mild traumatic brain injury: can we see the difference? *J. Neurotrauma* 30:2–10. <http://dx.doi.org/10.1089/neu.2012.2486>.
- Tournier, J.-D., Calamante, F., Gadian, D.G., Connelly, A., 2004. Direct estimation of the fiber orientation density function from diffusion-weighted MRI data using spherical deconvolution. *NeuroImage* 23:1176–1185. <http://dx.doi.org/10.1016/j.neuroimage.2004.07.037>.
- Tournier, J.D., Calamante, F., Connelly, A., 2007. Robust determination of the fibre orientation distribution in diffusion MRI: non-negativity constrained super-resolved spherical deconvolution. *NeuroImage* 35:1459–1472. <http://dx.doi.org/10.1016/j.neuroimage.2007.02.016>.
- Tournier, J.-D., Mori, S., Leemans, A., 2011. Diffusion tensor imaging and beyond. *Magn. Reson. Med.* 65:1532–1556. <http://dx.doi.org/10.1002/mrm.22924>.
- Tournier, J.D., Calamante, F., Connelly, A., 2013. Determination of the appropriate b value and number of gradient directions for high-angular-resolution diffusion-weighted imaging. *NMR Biomed.* 26:1775–1786. <http://dx.doi.org/10.1002/nbm.3017>.
- van der Horn, H.J., Kok, J.G., de Koning, M.E., Scheenen, M.E., Leemans, A., Spikman, J.M., van der Naalt, J., 2016. Altered wiring of the human structural connectome in adults with mild traumatic brain injury. *J. Neurotrauma* <http://dx.doi.org/10.1089/neu.2016.4659>.
- Veeramuthu, V., Narayanan, V., Kuo, T.L., Delano-Wood, L., Chinna, K., Bondi, M.W., Waran, V., Ganesan, D., Ramli, N., 2015. Diffusion tensor imaging parameters in mild traumatic brain injury and its correlation with early neuropsychological impairment: a longitudinal study. *J. Neurotrauma* 32:1497–1509. <http://dx.doi.org/10.1089/neu.2014.3750>.
- Vos, S.B., Jones, D.K., Viergever, M.A., Leemans, A., 2011. Partial volume effect as a hidden covariate in DTI analyses. *NeuroImage* 55:1566–1576. <http://dx.doi.org/10.1016/j.neuroimage.2011.01.048>.
- Wilde, E.A., McCauley, S.R., Hunter, J.V., Bigler, E.D., Chu, Z., Wang, Z.J., Hanten, G.R., Troyanskaya, M., Yallampalli, R., Li, X., Chia, J., Levin, H.S., 2008. Diffusion tensor imaging of acute mild traumatic brain injury in adolescents. *Neurology* 70:948–955. <http://dx.doi.org/10.1212/01.wnl.0000305961.68029.54>.
- Wilson, J.T., Pettigrew, L.E., Teasdale, G.M., 1998. Structured interviews for the Glasgow outcome scale and the extended Glasgow outcome scale: guidelines for their use. *J. Neurotrauma* 15:573–585. <http://dx.doi.org/10.1089/neu.1998.15.573>.
- Xu, J., Rasmussen, I.-A., Lagopoulos, J., Häberg, A., 2007. Diffuse axonal injury in severe traumatic brain injury visualized using high-resolution diffusion tensor imaging. *J. Neurotrauma* 24:753–765. <http://dx.doi.org/10.1089/neu.2006.0208>.
- Yoon, B., Shim, Y.S., Lee, K.S., Shon, Y.M., Yang, D.W., 2008. Region-specific changes of cerebral white matter during normal aging: a diffusion-tensor analysis. *Arch. Gerontol. Geriatr.* 47:129–138. <http://dx.doi.org/10.1016/j.archger.2007.07.004>.
- Yuh, E.L., Cooper, S.R., Mukherjee, P., Yue, J.K., Lingsma, H.F., Gordon, W.A., Valadka, A.B., Okonkwo, D.O., Schnyer, D.M., Vassar, M.J., Maas, A.I.R., Manley, G.T., Casey, S.S., Cheong, M., Dams-O'Connor, K., Hricik, A.J., Inoue, T., Menon, D.K., Morabito, D.J., Pacheco, J.L., Puccio, A.M., Sinha, T.K., 2014. Diffusion tensor imaging for outcome prediction in mild traumatic brain injury: a TRACK-TBI study. *J. Neurotrauma* 21:1–21. <http://dx.doi.org/10.1089/neu.2013.3171>.